Thermochimica Acta, 145 (1989) 101–114
Elsevier Science Publishers B.V., Amsterdam – Printed in The Netherlands

THERMAL ANALYSIS AND DSC: THE HYSTERESIS CYCLE IN SHAPE MEMORY ALLOYS

A. AMENGUAL, C. PICORNELL, R. RAPACIOLI,* C. SEGUÍ and V. TORRA
Departamento de Física, Universitat de les Illes Balears, E-07071 Palma de Mallorca (Spain)
(Received 9 August 1988)

ABSTRACT

The study of martensitic transformations in shape memory alloys by means of techniques such as unconventional scanning calorimetry, acoustic emission and optical microscopy has made it possible to establish the existing links between the hysteresis cycle and the internal state of a given material. We have studied the changes in the hysteresis cycle, concerning its shape, width and relevant temperatures, which are produced as a consequence of different thermal treatments and repetitive thermal cycling, for a Cu–Zn–Al single crystal. The effect of thermomechanical treatments in Cu–Zn–Al samples with different surface orientation is also studied. Relevant changes in a mixed hysteresis cycle (Cu–Al–Ni polycrystal with two martensite phases) are observed in annealing treatments. On the other hand, observation of the interfaces movement in reduced thermal cycling establishes the temperature scale and the geometrical conditions to obtain a repetitive/recoverable hysteresis cycle.

INTRODUCTION

It is well known that the martensitic transformation shows hysteretic behaviour [1]. The hysteresis loop for a complete transformation cycle gives a useful description of the macroscopic features of the transformation. In this sense the width of the hysteresis loop is thought to provide information about the frictional resistance to the interface motion, and the slope of the curves representing the transformed fraction of material versus temperature is related to the elastic energy stored/released in the sample as the forward/reverse transformation proceeds. The area enclosed by a "reversible" hysteresis loop drawn in the entropic diagram (temperature–entropy coordinates) obviously gives the heat released or the work lost in the cyclic process [2–4], and the changes produced in the hysteresis loop by cycling are related to irreversible processes taking place in the material which induces changes in the transformation path [5–7]. The thermoelasticity is explained only in

* Present address: Centro Atómico Bariloche and E.A. Escuela Superior Técnica, Cabildo 15, 1426 Buenos Aires, Republic of Argentina.

0040-6031/89/$03.50 © 1989 Elsevier Science Publishers B.V.

terms of elastic interactions between martensite plates [8]. Furthermore, mixed forms for the hysteresis loop are related to the coexistence of several martensite phases [2,9].

The aim of this paper is to study, by thermal analysis (unconventional DSC), acoustic emission or thermosonimetry (AE) and optical microscopy, the effects of the thermomechanical treatments on the global hysteresis cycle for a Cu–Zn–Al single crystal and the role that defects play in the transformation. The effect of thermal cycling, defect concentrations after heat treatments, annealing and different surface orientations (in previously mechanically cycled samples) have been studied. Besides these studies on global transformation cycles, local studies have been performed by means of simultaneous microscopic observations and acoustic activity detection, together with a high resolution temperature control. This allows one to determine, via the AE, the temperature resolution needed in order to obtain truly thermoelastic (recoverable) processes. In this case, the hysteresis loop for single martensite plates growing/shrinking in single crystal samples shows an "intrinsic" character with a fixed width.

EXPERIMENTAL

Two main experimental set-ups have been used. On the one hand, studies on global transformations have been performed using an unconventional differential scanning calorimeter (DSC) able to work in the range 80–400 K [6,10,11]. With the usual temperature scanning rates of about 0.3 K min^{-1}, the temperature resolution for the calorimetric signals (without signal processing) is about 0.01 K. Using semiconductor bismuth–telluride thermobatteries (MELCOR) the system allows one to detect transformation domains with a mass near 4 μg [12]. This device is especially appropriate to describe the transformation dynamics and is able to perform simultaneous coupled measurements of acoustic emission [13]. On the other hand, local studies in restricted temperature domains have been performed using an optical microscope, Olympus BH-2, (maximum magnification 700 $\times$, resolution near 1 μm) coupled with AE detection using standard techniques (ring-down counting and/or burst analysis). This experimental set-up [14–17] is temperature computer-controlled in order to achieve a resolution of about 0.003 K. The microscopic observations are stored in videomagnetic tape for further study.

Table 1 shows the nominal composition and Ms of the alloys used in this work.

The hysteresis loops are obtained representing extensive magnitudes, which we consider to be proportional to the transformed fraction of the sample, as a function of temperature for both the forward and reverse transformations. These extensive magnitudes are the relative enthalpy or

TABLE 1

Composition (at.%) and Ms (K) for the alloys used

Alloy	Cu	Al	Zn	Ni	Ms	
A	68.1	15.7	16.2	–	240	Single crystal
B	69.2	27.6	–	3.2	260	Polycrystal
C	68.5	16.2	14.9	–	285	Single crystal

entropy change for global transformation cycles, and the $\beta \leftrightarrow m$ interface position for partial thermal cycles.

RESULTS AND DISCUSSION

Global cycles

Thermal treatment and surface-state effects

Several disc-shaped samples of alloy A (6 mm diameter, thickness about 1 mm) were maintained for 10 min at 1123 K and then either cooled in air to room temperature (TT1) or quenched in ice water at 273 K (TT2). The thermal cycling between 200 and 300 K (largely including the Af to Mf range), at a mean temperature scanning rate (dT/dt) near 0.3 K min^{-1}, began 24 h after treatment in order to stabilize the reordering processes.

The hysteresis loops obtained for the first transformation cycle after the thermal treatments described above are shown in Fig. 1. The comparative analysis of the thermal energy released during the first transformation cycle after each heat treatment establishes that after TT1 the transformation starts with a sudden energy dissipation which takes place in a very narrow temperature domain. After that initial part, the transformation gradually progresses. On the other hand, after thermal treatment TT2, the transforma-

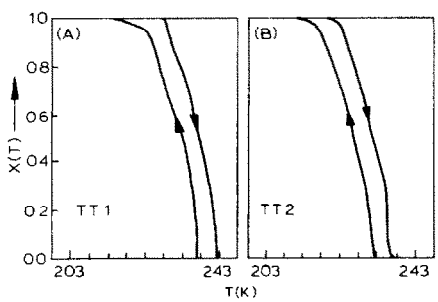

Fig. 1. Hysteresis loop in relative $\int dQ/T$ vs. T coordinates for the first transformation cycle: (A) after TT1 and (B) after TT2.

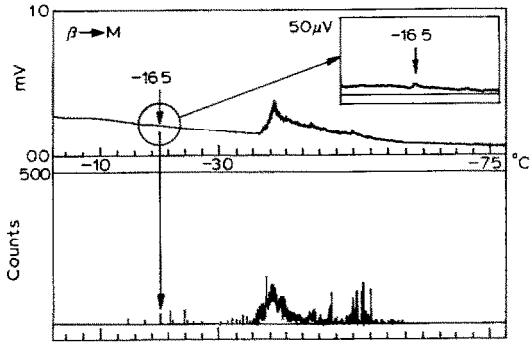

Fig. 2. Thermogram corresponding to the $\beta \rightarrow m$ transformation in the first cycle after TT2, showing the correlation between acoustic peaks and small calorimetric dissipations at temperatures far above the nominal Ms.

tion starts with small calorimetric pulses at higher temperatures than Ms(TT1) (more than 20 K) [6], as can be seen in Fig. 2. These calorimetric pulses would correspond to elemental transformations of about 30 μg of material, energy about 180 μJ, which are virtually at the limit of our resolution, then being unobservable at the usual calorimetric working scale (standard DSC resolution near 1 mg). The simultaneous AE detection in the usual scale shows correlated bursts, as can also be seen in Fig. 2. After that, the transformation starts with an increasing mean growing in all the transformation temperature domain. The temperature extension and the hysteresis width of both the $\beta \rightarrow m$ and $m \rightarrow \beta$ transformations are larger after TT2 than after TT1.

The microscopic observations of the transformation agree with the obtained behaviour. After TT1 the transformation starts with the fast growth of big martensite plates, while after TT2 it starts with the simultaneous growth of a lot of small plates, which need a continuous decrease of temperature for further growth. This want of continuous increase of thermodynamic driving force is related to the mechanical interaction between plates.

If the surface state of a sample is changed by different degrees of polish (mechanical or electrolytic polish) after thermal treatment TT1, it is observed that the better the surface state, the higher is the difference Ms – Af. At the same time, the material fraction which transforms within the initial part of the transformation (only 2 K), also increases, as can be seen from Fig. 3 and from Table 2. As will be discussed later, these features are related to the increase in critical driving force for nucleation associated with the lowering of Ms in the first cycle after TT1.

The different features observed in the first cycle after each thermal treatment can be associated with different concentrations of defects in the material after each treatment.

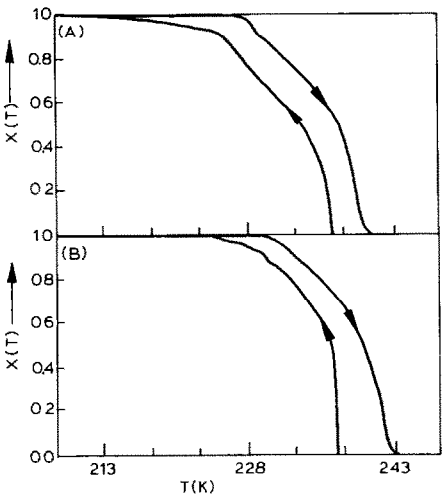

Fig. 3. Hysteresis loops in relative $\int dQ/T$ vs. T coordinates obtained in the first cycle for the same sample: (A) mechanically polished before TT1 and (B) electrolytically polished before TT1.

(1) The higher concentration of defects created and frozen by water-quenching (TT2) favours the martensite nucleation/growth of martensite at higher temperatures and in several places.

(2) If one assumes that Ms is the temperature at which the bulk transformation starts, it can be stated that Ms(TT1) > Ms(TT2). This effect can be explained by the different mean-order parameter value. The higher quenching rate in TT2 leads to a lower mean-order parameter [18,19].

(3) The higher amount of defects present in the sample after TT2 produces more frictional work, increasing the hysteresis width. Optical microscopy observations show a large number of martensite plates with important interactions between them. The appearance of a large amount of plates prevents the transformation progress, so increasing the temperature extension. The large elastic interactions between interfaces in this case play a very important role in the enlargement of the temperature extension of the transformation.

(4) As can be observed from Fig. 3, the explosivity of the onset of the first forward transformation increases when reducing the surface relief. That is,

TABLE 2

Sample fraction transformed within the range Ms to (Ms + 2) K (in %) and Ms–Af difference (in K) in the 1st cycle after TT1 for mechanically and electrolytically polished samples

	x (%)	Ms–Af
Mechanical polish	20.0	4.7
Electrolytic polish	41.2	7.3

the fraction of material which transforms non-thermoelastically increases, so a more important part of the sample transforms with a great irreversibility. The fast interface movements which can be associated with this initial behaviour create new defects.

(5) An easier nucleation (at a higher Ms) is observed when the sample has a worse surface state. The defects will serve as nucleation sites if they have a favourable orientation relative to the surface. Irregularities in the surface favour a large number of defects having this favourable orientation.

(6) If a sequence of thermal treatments followed by thermal cycling is performed on the sample (namely TT1–TT2–TT1 or TT2–TT1–TT2) different behaviours can be observed for each sequence. This means that, although the thermal treatment strongly influences the subsequent transformation, some characteristics of the previous thermal treatments remain in the sample.

Cycling effects

Figure 4 shows the hysteresis loops corresponding to the first and second transformation cycles for a sample submitted to thermal treatment TT1. As can be seen in this figure, $Ms(1) < Ms(2)$, while the other transformation temperatures remain almost constant. Consequently, $|Ms(1)-Af(1)| > |Ms(2)-Af(2)|$, this effect being more pronounced, the better the surface state.

In further thermal cycling after TT1 an enlargement of the hysteresis width is observed from cycles 2 to 10, as can be seen from Fig. 5, which shows the hysteresis loops for the second and tenth cycles after TT1. A larger shift of the forward transformation curve with respect to the reverse one is responsible for this enlargement. Conversely, the hysteresis cycle does not experience any important change by cycling after TT2 [20]. The width of the hysteresis loop also increases by fast thermal cycling (between baths at 293 K and 200 K) from the 11th up to the 99th cycles for both TT1 and TT2.

According to the above observations, the following can be established.

(1) If the surface relief is removed by electrolytic polish, the first forward transformation after TT1 starts in a very explosive way. This non-thermo-

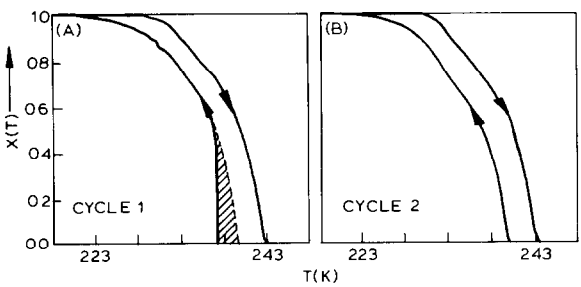

Fig. 4. Hysteresis loops for the first (A) and second (B) transformation cycles after TT1.

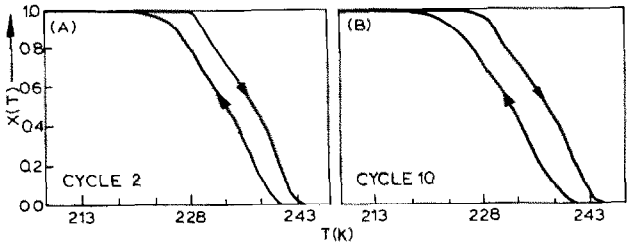

Fig. 5. Hysteresis loops for the second (A) and tenth (B) transformation cycles after TT1.

elastic transformation, related to high speed interface movements, generates a large number of defects. The explosive character of the begining of the direct transformation is lost in the second cycle. This feature makes the area enclosed by the hysteresis loop higher for the first than for the second cycle (lined area in Fig. 4).

(2) The shift of Ms between the first and second cycles, while Mf, As and Af remain almost constant, reveals that a particular effect occurs in the first cycle. This behaviour is related to a delay of the "first nucleation" in the air-cooled samples. It has been pointed out [5] that this nucleation delay is due to the absence of defects, able to be nucleation sites, after the air cooling. During the first transformation cycle new defects are created which favour the nucleation in the second cycle. As a matter of fact, optical microscopy observations show that the transformation starts at different places in the sample in the first and following cycles, always starting at the sample edges.

(3) The enlargement of the hysteresis width after ten cycles can be related to an increase of the frictional terms. The defects created by thermal cycling (mostly clusters of dislocations) are responsible for this frictional work. A different shift in $\beta \rightarrow m$ and $m \rightarrow \beta$ transformations indicates that different frictional mechanisms exist in both cases.

Annealing treatments (Cu–Al–Ni)

By quenching samples of alloy B to room temperature, two phases, namely the orthorhombic β_1' and the hexagonal γ_1' were observed to coexist in the martensitic state, instead of the expected, γ_1'. This results in a mixed hysteresis loop, as can be seen in Fig. 6. Similar behaviour was observed by Otsuka et al. [9] for stress-induced transformation in Cu–Al–Ni alloys. The appearance of the β_1' phase is closely related to the high internal stresses (revealed by a great temperature extension) built up in the sample as a consequence of the γ_1' growth [21]. The β_1' martensite progressively disappears after the samples are annealed for variable times at 200 or 300 °C, as is also shown in Fig. 6. Along with this feature, an increase in slope and a decrease in hysteresis width can be observed when the annealing time increases.

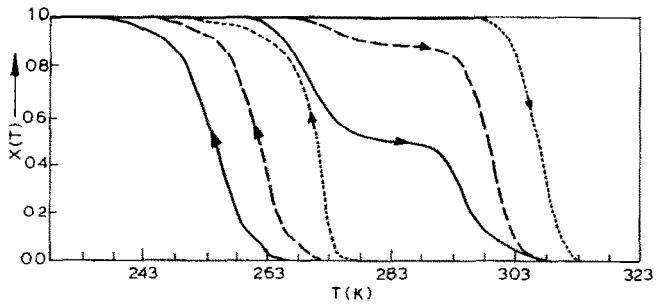

Fig. 6. Hysteresis loops obtained after different annealing times at 573 K: $t = 0$ (———), $t = 22$ s (— — —) and $t = 55$ s (· · · · · ·).

(1) The strongly discontinuous character of the $\beta_1 \rightarrow \gamma_1'$ transformation contributes to the enhancement of the hysteresis width. Annealing acts in two ways: on the one hand, by ordering processes, it increases the transformation temperatures; on the other hand, it decreases the concentration of quenched-in defects making the γ_1' growth smoother, leading to the suppression of the β_1' phase and to a more reversible transformation path. As a consequence, both the slope increases and the hysteresis width diminishes.

Thermomechanical treatments

Samples of alloy A were submitted to a training process by means of repetitive mechanical cycling, which leads to the preferential formation of one or a few martensite variants. After that, they were cut in different orientations relative to the habit plane. Calorimetric and acoustic detection was performed in thermal cycles betwen 203 and 293 K, both before and after removing the training effect by maintaining the samples at 1123 K for 6 h. The resulting hysteresis cycles are shown respectively in Figs. 7 and 8.

Observations of different cycles were carried out by means of optical microscopy. Those samples parallel to the habit plane show a single-variant transformation while in the other samples two or more variants appear, one

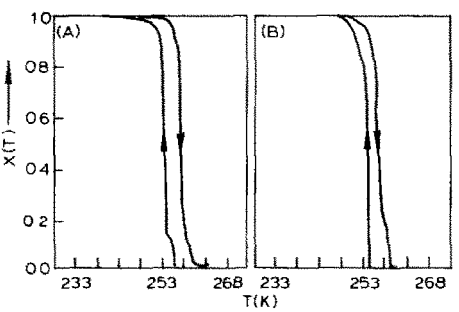

Fig. 7. Hysteresis cycles obtained for a sample cut parallel to the habit plane: (A) before and (B) after thermal treatment.

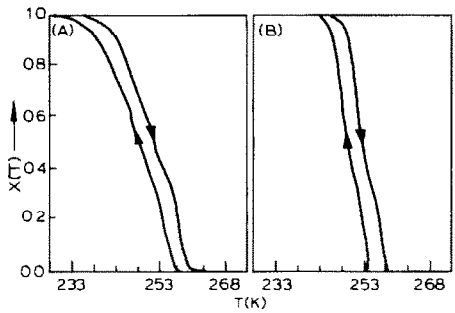

Fig. 8. Hysteresis loops obtained for a sample cut non-parallel to the habit plane: (A) before and (B) after thermal treatment.

of them being the "trained" one. After the thermal treatment, other variants appear, but the mechanically induced variant was still present in all samples.

Our results show the following:

(1) The surface orientation plays a definitive role in the transformation dynamics. Different transformation dynamics were obtained for each cut orientation. Those samples cut parallel to the habit plane show an almost vertical hysteresis loop, as expected for a single-variant transformation where no elastic energy is stored/released. On the other hand, a lower slope for the transformation curves in samples cut non-parallel to the habit plane can be related to the interaction between different variants.

(2) The discontinuous, burst type, progress of single-variant transformation in samples cut parallel to the habit plane shows the important role that defects play in transformation dynamics. The hysteresis width can be associated with these defects. A higher acoustic emission detected in this case compared with that of samples non-parallel to the habit plane can be associated, as we shall see, with these defects acting as pinning centres. The hysteresis width for samples cut parallel to the habit plane decreases after thermal treatment, as a consequence of the elimination of the preferentially oriented defects inserted by mechanical cycling.

The slope of the hysteresis curves for samples non-parallel to the habit plane increases after thermal treatment, reflecting the relaxation of the interactions between variants (the spontaneous transformation minimizes the stresses by self-accommodating variants growth).

Local studies

Studies on partial thermal cycling were performed by means of AE detection coupled with optical microscopy observations. These local studies concern growth and shrinkage of martensite single plates either with or without loading of the sample with a weak external traction. Thermal

cycling in restricted conditions (reduced temperature interval and accurately controlled extremes of temperature and temperature rates) allows us, on the one hand, to observe and also to record on video-magnetic tape the evolution of the martensite-matrix interfaces; the interface position can be plotted as a function of temperature to obtain an alternative representation of the hysteresis loop. On the other hand, acoustic emission is a very sensitive tool for detecting material changes.

The results show the relationship between the appearance, growth, shrinkage and motion of martensite plates with the acoustic signals monitored, and are also able to quantify the transformation recoverability in consecutive thermal cycling.

Recoverable / stochastic character

(1) It is possible to obtain reproducible transformations by cycling when the sample is under stress if the temperature control is better than 0.01 K. Small changes in the temperature domain produce relevant changes in the acoustic activity (temperature distribution and intensity of the acoustic signals.) This means that uncontrolled temperature cycling makes the transformation paths non-reproducible, so the sample does not recover its initial state after each cycle.

Comparison of the AE obtained for spontaneous or stress-aided cycling shows that a higher temperature resolution is needed in spontaneous transformation (which can be evaluated as 0.01 K divided by 24 available martensite variants) to obtain reproducible AE patterns for the transformation. The temperature resolution can be interpreted as a certain extent of irreversibility acting on the sample. From the Fourier equation, the thermal diffusion of a heat pulse produced at $r = 0$ in $t = 0$ can be determined. After Δt, the region of material with homogeneous temperature is a sphere with radius r, given by

$$r^2 = 6D\Delta t = 6D\Delta T/(\mathrm{d}T/\mathrm{d}t)$$

We can see that for each thermal diffusion coefficient (D) and given temperature rate ($\mathrm{d}T/\mathrm{d}t$), the mean distance at which the perturbation becomes homogeneous depends on the temperature resolution needed. So the smaller the introduced irreversibility (ΔT), the greater the length of sample that is non-perturbed. That is, for each material and length, a temperature scale is available to obtain recoverable consecutive thermal cycles.

(2) Previous results [22] show that the acoustic emission is directly related to the sudden release of energy after the interface overcomes a finite energy barrier which opposes its motion. These energy barriers can be due to the existence of defects in the sample or to the appearance, disappearance or changes of other martensite variants.

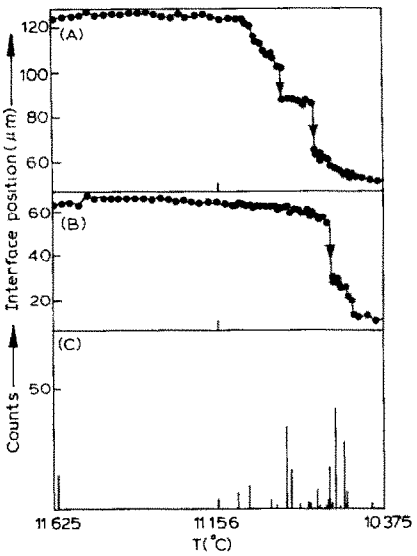

Fig. 9. Evolution of the interface position as a function of decreasing temperature and associated acoustic emission: (A) plate 1, (B) plate 2 and (C) acoustic emission.

Intrinsic hysteresis

(1) As mentioned above, the plot of the interface position versus temperature gives an alternative representation of the hysteresis loop [22]. It has been observed that the interface movement can stop and then suddenly continue, an AE signal then being detected, as can be seen in Fig. 9. In fact, the cessation of interphase motion is a cause for the hysteresis width to increase as can be seen in Fig. 10. The increase of the hysteresis width, as well as the AE intensity, are indicative of the instability due to the potential barrier that has to be surmounted. The energetic barriers, which behave asymmetrically for the forward and reverse transformation, can have different energy levels and slopes, depending on their origin, and, in this sense,

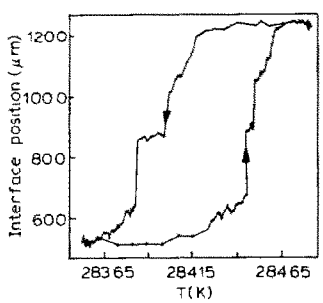

Fig. 10. Hysteresis loop in interface position vs. temperature coordinates obtained for a single martensite plate during partial cycling.

the higher the instability, the higher is the local hysteresis width, and a more intense AE has to be expected.

Parallel optical microscopy observations were made in samples with a certain amount of stabilized martensite, where only restricted domains of β-phase exist between plates of stabilized martensite. These observations show the same hysteresis behaviour concerning the hysteresis width.

(2) Besides this contribution, the hysteresis loop has an intrinsic character, which, at low rates, is temperature and temperature-rate independent. That is, it shows an intrinsic width, of about 0.5 K, which is not due to any internal evolution. In this sense, there exists an energy barrier between the two coexistent phases that must be taken into account together with the other frictional and interactional contributions (discontinuous or pinning–unpinning processes), bursts or local energy barriers producing the transformation hysteresis. Furthermore, the hysteresis loop for a single martensite plate shows a finite slope (about 100 μm K^{-1}) which points out that a continuous thermodynamic driving force has to be provided in order to move the interphase even when there are no external elastic interactions. The finite slope can be related to local composition/ordering changes or internal stresses produced by accumulative interface-bulk interactions.

CONCLUSIONS

(1) The temperature extension, that is, the slope of the transformation curves, is determined by the interaction between variants. The hysteresis width is built up of different contributions: intrinsic hysteresis, friction phenomena and pinning–unpinning processes (such as nucleation and interactions between interfaces and defects).

The part of the hysteresis loop which corresponds to a non-thermoelastic growth of martensite depends on the surface state of the sample: the higher the amount of defects present in the surface, the smaller the non-thermoelastic part of the transformation, will be, as well as the number of defects created.

(2) If the initial concentration of defects is relatively high, the transformation starts showing small calorimetric and acoustic bursts at temperatures far above the nominal Ms.

(3) AE detection is much more sensitive than other parameters, so the detection of AE signals when no changes are detected in other measured magnitudes does not mean that AE is not related to the transformed mass. Comparison between AE and other parameters, such as resistivity, can lead to wrong interpretations. Our observations establish that the detected AE is associated with accelerations in the growth/shrinkage of the martensite phase.

(4) Intense discontinuous transformations generate new defects. Furthermore, important internal stresses can be induced in the material leading to the formation of different martensite phases. For jerky transformations, the distribution of bursts in temperature has to be maintained in order to attain reversible transformations. In terms of calorimetric or acoustic peaks this means that they must be distinguishable and well separated. For spontaneous transformations in dimensions of about 1 cm, this presupposes a rigorous temperature control and a very low temperature rate.

(5) The recoverability of the transformation is lower as more causes exist for irreversibility and the creation of defects. These causes can be the temperature rate, the number of available martensite variants and the size of the samples. Using samples with partially stabilized martensite, the diminution of the β-phase domains could contribute towards a more controlled spontaneous evolution of the material.

ACKNOWLEDGEMENTS

The present work has had financial support from the CAICYT (research project no. 3562/83) and from the CICYT (project PA 86-0079). R.R. acknowledges a sabbatical year (1986–87) from CAICYT. Enlightening discussions about some parts of this work from F.C. Lovey and M. Ahlers (Centro Atómico Bariloche, Republic of Argentina) are gratefully acknowledged. The authors also wish to thank the Dep. Metaalkunde of the K.U. Leuven for kindly providing Cu–Al–Ni alloys.

REFERENCES

1 L. Delaey and E. Aernoudt, Proc. Conf. ICOMAT 86, Nara, Japan, Jpn. Inst. Met., 1986, pp. 926–933.
2 L. Delaey, J. Ortín and J. Van Humbeeck, Proc. Int. Conf. on Phase Transformations, Cambridge, England, 1987, The Institute of Metals, 1988, pp. 60–66.
3 J.M. Vidal, Prof. R. Marqués in memoriam, Faculty of Physics, University of Barcelona, 1981, pp. 421–428.
4 J. Ortín and A. Planes. Acta Met. Overview, 68 (1988), 1873.
5 C. Picornell, C. Seguí, V. Torra and R. Rapacioli, Scr. Metall., 22 (1988), 999.
6 C. Picornell, Thesis, Universitat Illes Balears, 1987.
7 F.C. Lovey, E. Cesari, V. Torra and J.M. Guilemany, Mater. Lett., 5 (1987) 159.
8 R.J. Salzbrenner and M. Cohen, Acta Metall., 27 (1979) 739.
9 K. Otsuka, C.M. Wayman, K. Nakai and H. Sakamoto, Acta Metall., 24 (1976) 207.
10 C. Picornell, C. Seguí, V. Torra, J. Hernáez and C. López del Castillo, Thermochim. Acta, 91 (1985) 311.
11 H. Tachoire, J.L. Macqueron and V. Torra, Thermochim. Acta, 105 (1986) 333.
12 J. Ortín, V. Torra and H. Tachoire, Thermochim. Acta, 121 (1987) 333.

13 C. Picornell, C. Seguí, V. Torra, C. Auguet, Ll. Mañosa, E. Cesari and R. Rapacioli, Thermochim. Acta, 106 (1986) 209.
14 C. Picornell, C. Seguí, V. Torra, F.C. Lovey and R. Rapacioli, Thermochim. Acta, 113 (1987) 171.
15 F.C. Lovey, J. Ortín and V. Torra, Phys. Lett. A., 121 (1987) 352.
16 A. Amengual, Ms. Thesis. Dept. Física, Universitat Illes Balears, 1987.
17 Ll. Mañosa, C. Picornell, C. Seguí and V. Torra, J. Acoustic Emission, 5 (1986) S49.
18 A. Planes, J. Viñals and V. Torra, Philos. Mag. A, 48 (1983) 501.
19 J. Viñals, Thesis, Universitat de Barcelona, 1983.
20 C. Picornell, R. Rapacioli, C. Seguí and V. Torra, Rev. Métall. 9 (1987) 491.
21 Y. Nakata, T. Tadaki and K. Shimizu, Trans. Jpn. Inst. Met., 26 (1985) 646.
22 A. Amengual, F. Garcias, F. Marco, C. Seguí and V. Torra, Acta Metall., 36 (1988) 2329.